06

Calorimetric study of Al−xSi−2 wt% Cu silumin with 15, 17 and 20 wt% silicon

© P.N. Yakushev, V.N. Osipov, V.A. Bershtein, S.P. Nikanorov

Ioffe Institute,
194021 St. Petersburg, Russia
e-mail: yak@pav.ioffe.ru

Received March 30, 2023
Revised July 11, 2023
Accepted July 14, 2023

Effect of a solidification rate and silicon content on aluminum silicon eutectic and intermetallic phase of Al−Si−Cu-alloys by differential scanning calorimetry is studied. Ultimate tensile strength of the alloy is analyzed on the base of observed microstructure and volumes of phases, estimated from the measured values of the melting enthalpy.

Keywords: alloy microstructure, differential scanning calorimetry, eutectic and intermetallic phases.

DOI: 10.61011/TP.2023.09.57361.63-23

Introduction

Hypereutectic silumins are widely used in the automotive industry in the manufacture of pistons, liners in internal combustion engines, diesel parts and other devices. Strict operational requirements to them initiate wide research of microstructure and its influence on strength, ductility and other physical and mechanical properties of silumins.

Various methods of modifying the structure of molded silumin [1] are being investigated. The effect of the amounts of introduced chemical elements on the modification of eutectic and primary silicon crystals of Al−Si−Cu [2,3] ternary alloys is investigated. Ternary silumins with copper and magnesium are effectively modified by heat treatment and aging. The application of such modification in practice and studies of its different variants lead to an increase in strength [4,5]. It is also known to improve the strength properties of ternary silumins when solidified at an increased rate. Thus, at the low cooling rate of Al−14% Si−2.6% Cu with Ce [2] addition, the crushing of primary silicon crystals and the formation of ternary compound Al−Si−Cu were observed. Increasing the cooling rate resulted in simultaneous modification of primary and eutectic silicon. In [5] work, the effect of high solidification rates on the structure and strength properties of Al−Si−Cu-alloy has been investigated. When cast in a sand crucible, the cooling rate was 14.5°C/s, when the rod was pulled from the melt and cooled by water drops — 201.5°C/s. In the first case, needle-shaped binary eutectic suspended in α-Al matrix and ultimate tensile strength up to 250 MPa were observed, while in the second case — thin spherical eutectic and α-Al dendrites and strength up to 350 MPa were observed. However, it was noted in [6] that porosity increases in alloys grown at high cooling rates.

In the works [7] the process of obtaining a hypereutectic Al−Si alloy with a fully eutectic sub-fibrous structure by directional solidification with such an increased solidification rate, which ensures the shift of the eutectic point towards increasing silicon content to the selected alloy composition, was considered. The alloy crystallization was carried out by pulling the sample out of the melt through an air-cooled molder using the Stepanov [8] method. Solidification was investigated at 1 mm/s, corresponding to a cooling rate of about 10°C/s. The alloy had increased ultimate tensile strength (UTS) and record high elongation at fracture (ε_L). It has been shown that the alloy with a fine fiber structure exhibits high efficiency in addition to improving physical and mechanical properties by chemical modification.

It seemed important to apply this approach to improve the properties of commercial ternary silumin Al−Si−Cu, i.e. to obtain a three-component alloy with optimal content and fine structure of the eutectic phase αAl + Si, shifted towards higher silicon content up to the quasi-eutectic point by increasing the solidification rate. However, there is currently no diagram of the structure of Al−Si−Cu phases as a function of silicon content and cooling rate, which would allow the selection of conditions for obtaining the optimum eutectic content in the alloy. Therefore, the present work investigated the effect of silicon content and solidification rate on the eutectic phase in the ternary alloy.

1. Material and research techniques

In the present work, an alloy close in composition to AK12M2MgN grade was used. Ribbons with a length of about two meters and a cross section of 10 × 2 mm were drawn from the melt in a graphite-chamotte crucible through an shaper instead of molder using the Stepanov method. To increase the silicon content above 12.5 wt.% (eutectic composition of binary aluminium-silicon alloy), additional silicon was introduced into the melt. The melt was incubated for 3 h at 800°C with periodic stirring before

Table 1. Composition of investigated alloys in weight units (wt.%)

Al	Mg	**Si**	Ti	Mn	Fe	Ni	**Cu**	Zn
74.6	0.80	**14.6**	0.3	0.5	1.2	1.1	**2.5**	0.6
74.5	0.9	**17.4**	0.1	0.4	0.7	1.08	**2.3**	0.4
71.8	0.5	**20.1**	0.2	0.5	1.3	0.8	**1.9**	0.3

each tape drawing. Pulling was performed at 660°C at a rate of 0.1 or 0.8 mm/s. The composition of the samples is given in Table 1.

The silicon content exceeded the initial content due to liquation by 2 wt.%. Therefore, sample composition measurements were performed repeatedly on the side surfaces of the tapes by electron diffraction spectroscopy (EDS). In addition, the silicon content of both the lateral surface of the tape and the cross sections was measured by electron optical method. Additionally, the silicon content was measured on the facet and on the fine chips of the material. The average error of composition measurement due to measurements at different points of the samples and by different methods did not exceed 3%. Hereafter, the samples of the three compositions will be designated by the composition of the main elements as: Al–15 wt.% Si–2 wt.% Cu, Al–17 wt.% Si–2 wt.% Cu, Al–20 wt.% Si–2 wt.% Cu.

In addition, Al–15 wt.% Si samples previously grown by the same method from molten aluminium and silicon of technical purity (99.85 and 99.9 wt.% respectively) at a directional solidification rate 1 mm/s corresponding to a cooling rate of approximately 10°C/s [7] were used.

For calorimetric measurements, samples of about $2 \times 2 \times 1$ mm were cut from tapes with silicon contents of 15, 17, and 20 wt.%. The analysis was performed by differential scanning calorimetry (DSC) using a DSC 6300 calorimeter from Seiko Instruments (Japan). Measurements of heat fluxes dependence on temperature were carried out at heating and cooling rates of 10 K/min. The temperature ranges and enthalpies of structural transformations — endothermic decomposition (melting) of eutectic phase ΔH_m and exothermic process of eutectic formation (crystallization) during melt cooling ΔH_{cr} were determined.

2. Results and discussion

The microstructure and strength of the same specimens were investigated earlier in our work [9]. Here, the basic summaries necessary to analyze the results of the DSC studies are given.

The structure of samples with different silicon content obtained by the Stepanov method at different solidification rates is shown in Fig. 1. Three main phases can be seen: α-Al dendrites (white), αAl + eutectic, βSi (black) and intermetallic compounds (grey). The elemental composition of these phases was determined by us earlier [9]. It can be seen that with the increase of the solidification rate of the alloys of both compositions, the flake structure of the eutectic is transformed into a fibrous one, with the fiber diameter decreasing to the size not resolvable by optical microscope (Fig. 1, *a, b* for the alloy with 15 wt.% Si and Fig. 1, *c, d* for 20 wt.% Si). Increasing the silicon content at a constant solidification rate (Fig. 1, *a, c* for 15 wt.% Si and Fig. 1, *b, d* for 20 wt.% Si) does not cause a noticeable change in phase morphology. There is, however, a slight increase in the volume of α-Al due to a decrease mainly in the volume of the eutectic. This effect was detected in our previous work [9] by measuring the phase areas in the sample cross-section as a percentage. When the silicon content increased from 15 to 20 wt.%, the area of α-Al increased from 49 to 56%, and the area of eutectic decreased from 45 to 38%, the rest — intermetalloides. The structure of the Al–15 wt.% Si binary alloy samples obtained earlier at a growth rate of 1 mm/s [7] on the same setup used to grow the Al–Si–Cu alloys under consideration is shown in Fig. 2. The alloy has a fully eutectic α Al + Si structure without α-Al solid solution crystals and primary Si crystals. The eutectic has a point flake structure. This is due to the fact that at a growth rate of 1 mm/s, the eutectic point of the Al–Si alloy shifts from 12.5 to 15 wt.%% Si [7].

Fig. 3 shows the results of measuring the temperature dependences of heat flux power in the calorimeter during heating and cooling at a rate of 10 K/min of the alloys Al–15 wt.% Si–2 wt.% Cu and Al–15 wt.% Si.

The DSC of binary Al–15 wt.% Si alloy grown at a cooling rate of 0.8 mm/s shows one endothermic peak upon heating with a maximum at 593°C and an exothermic peak with a maximum at 555°C. These peaks correspond to the melting and crystallization of – solidification of the eutectic αAl + Si. There are no other phases here. When the Al–15 wt.% Si–2 wt.% Cu sample was heated, two peaks were observed, at 544 and 577°C, and a little noticeable kink around 560°C. In the case of cooling, a peak at 545°C and a trace of the peak at about 520°C are visible. Thus, it can be stated that the peaks at 593 and 555°C in the curves of Fig. 3 correspond to the melting and solidification of αAl + Si eutectic phase of Al–15 wt.% Si-alloy, a peaks at 577 and 545°C — melting and solidification of αAl + Si eutectic phase of three-component alloy Al–15 wt.% Si–2 wt.% Cu. This is consistent with previously published DTA- and DSC studies of Al–Si and Al–Si–Cu in papers [4,10–13].

The DSC heating curves of ternary alloy Al–11 wt.% Si–*x* Cu–0.3 Mg at $x = 1.2$ and 3 wt.% were investigated in [14] and discussed in the review [13]. The endothermic effect curve of Al–11 wt.% Si–3 wt.% Cu has the same character as the Al–15 wt.% Si–2.5 wt.% Cu alloy studied here (Fig. 3). In paper [14], peaks at 575°C with a height of about 4 W/g and about 540°C with a height of 1.5 W/g were observed. The first peak was explained by melting of α-Al + Si(+Al_5SiFe + ...) = Liq. In the present paper, the first peak at 577° has a height of 3.5 W/g, the

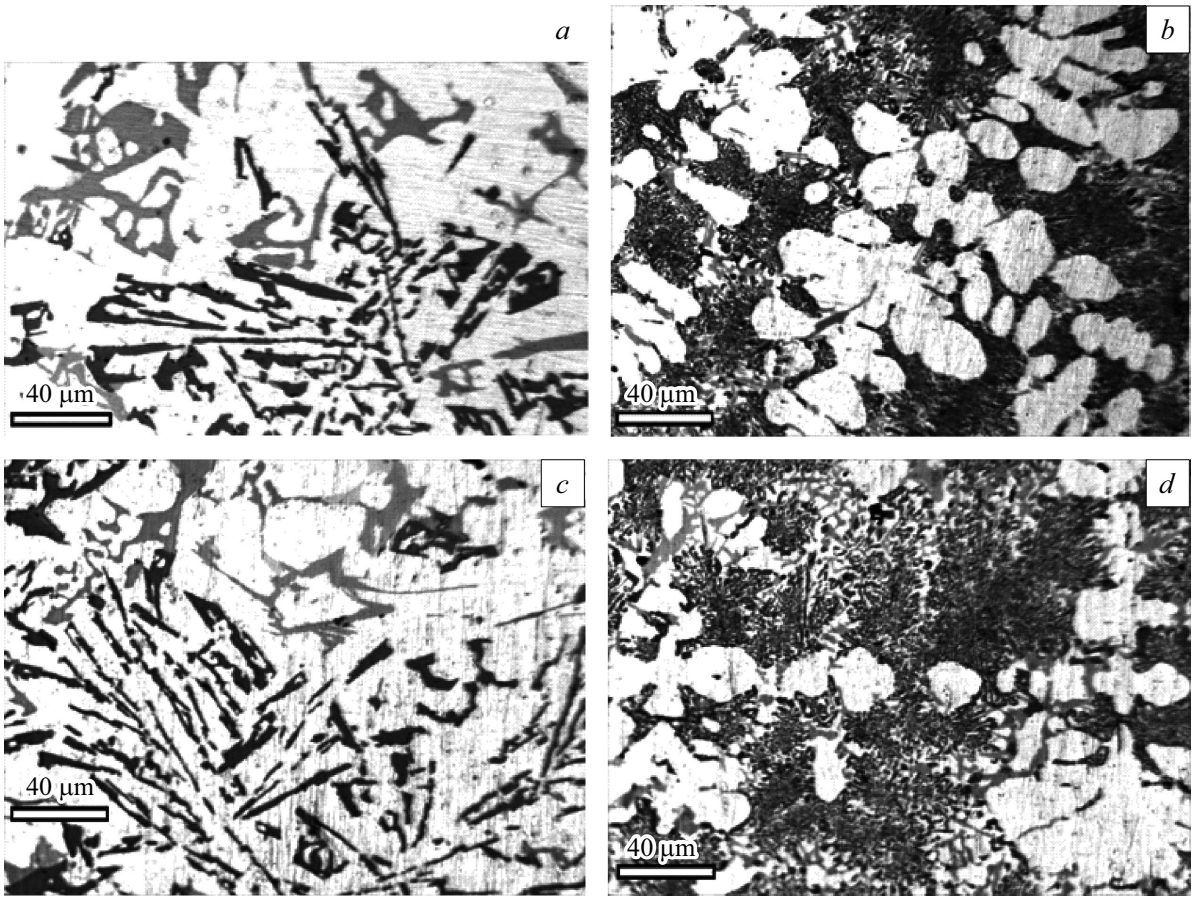

Figure 1. Microstructure of Al–15 wt.% Si–2 wt.% Cu alloy at solidification rate: *a* — 0.1, *b* — 0.8 mm/s; and Al–20 wt.% Si–2 wt.% Cu at solidification rates: *c* — 0.1, *d* — 0.8 mm/s.

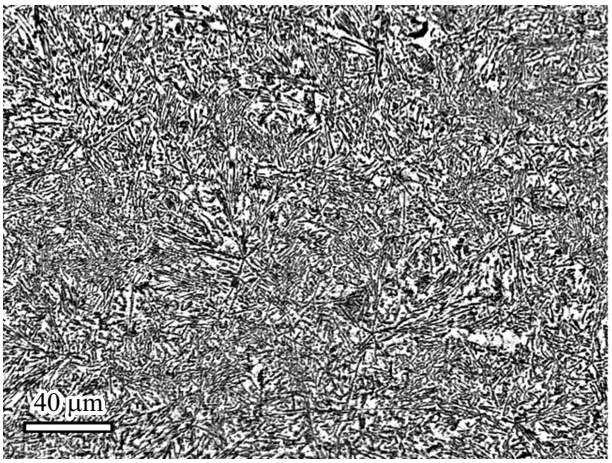

Figure 2. Structure of alloy Al–15 wt.% Si at solidification rate 1 mm/s.

second peak at 544°C — high about 1 W/g (Fig. 3). There is a good match between the results and those of [14].

Fig. 3 also shows the value of the total enthalpy of crystallization ΔH_{cr} and enthalpy of melting ΔH_m of the eutectic with associated intermetallic compounds of Al–15 wt.% Si–2 wt.% Cu and Al–15 wt.% S eutectic, respectively, determined from DSC measurements. We can compare the internal heat of fusion of an Al–15 wt.% Si alloy, consisting of only one eutectic phase and equal to

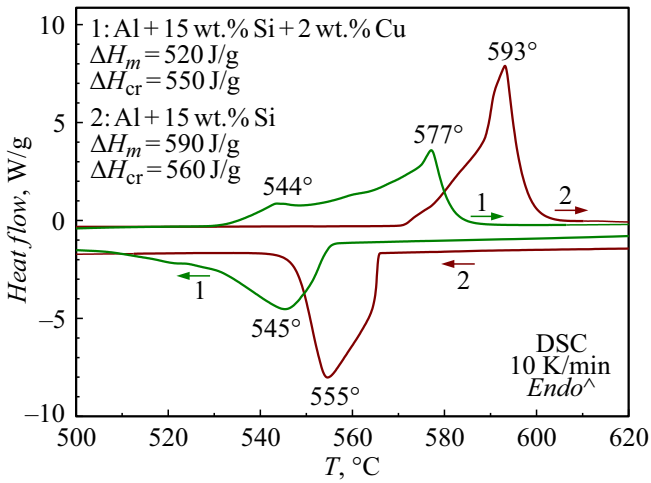

Figure 3. Temperature dependence of the heat flux in the calorimeter during phase transformations of Al–Si and Al–Si–Cu. The enthalpies of melting ΔH_m and crystallization ΔH_{cr} are given.

Table 2. DSC data for samples of mass m of Al−xSi−2 wt.% Cu alloys obtained at solidification rate V (scan rate 10 K/min)

Sample number	Sample parameters			First scan				Second scan			
				Melting		Solidification		Melting		Solidification	
	V, mm/s	xSi, wt.%	m, mg	T_{max}, °C	ΔH_m, J/g	T_{max}, °C	ΔH_{cr}, J/g	T_{max}, °C	ΔH_m, J/g	T_{max}, °C	ΔH_{cr}, J/g
1	0.1	15	64	576	525	545	545	578	510	546	550
2	0.8	15	48	577	520	545	550	576	520	537	550
3	0.1	17	40	576	545	546	600	573	555	546	590
4	0.8	17	54	577	530	543	580	575	560	543	580
5	0.1	20	54	577	580	547	610	575	590	547	620
6	0.8	20	48	577	580	546	610	574	600	546	630

590 J/g, with the total latent heat of fusion of an alloy of the same composition 540 J/g (Fig. 8 of work [14]). The difference is not much greater than the average error of measurement of this value by DSC and DTA methods for Al−20 wt.% Si alloy samples with different impurity content according to the works [11–14].

In the present work, DSC studies were performed on six Al−Si−Cu alloy samples with different silicon contents — 15, 17, and 20 wt.%, obtained at growth rates of 0.1 and 0.8 mm/s. The nature of the DSC dependence is similar to that observed for the alloy Al−15 wt.% Si−2 wt.% Cu in Fig. 3. The temperatures of T_{max} maxima at the melting and crystallization peaks of the α Al + Si eutectic, as well as enthalpies of phase transitions — the formation of eutectics and intermetallic compounds during crystallization of ΔH_{cr} in the area of 510−555°C and melting of ΔH_m in the area from 530 to 585°C, have been determined from these measurements. The results are shown in Table 2.

The difference in the T_{max} of melting and solidification of all alloys is approximately the same. It is related both to the inertia of temperature change and to the different nature of the process, since solidification occurs when the melt is supercooled.

The data in the table show that the T_{max} of melting and T_{max} of solidification of the eutectic, determined at a scan rate of 10 K/min, are independent of the solidification rate of the original alloy (0.1 and 0.8 mm/s). At the same time, the total enthalpies of melting and crystallization, given in Table 2, clearly increase with increasing silicon content in the alloys, although this does not reflect the processes occurring in different phases.

In order to analyze in more detail the obtained complex melting peaks of the studied samples, we attempted to decompose them into their components (Fig. 4, 5). The heat flux energy is determined from the time dependence of the heat flux. In these coordinates, the optimal ratio of areas and shapes of the peaks of the decomposition into DSC spectra is given by the bigauss approximation. In this case, the shape and area of the cumulative curve (sum of peaks) maximally coincide with the DSC curve (Fig. 4, 5).

Identification of the separated melting peaks on DSC curves was made by comparison with the peak temperatures of alloys with close chemical compositions (found by DSC and DTA differential thermal analysis methods [14–16]) and consideration of phase diagrams for five- and six-component alloys [16]. The following are taken as the most probable phases responsible for the manifestation of the observed peaks:

peak 1 — eutectic αAl + Si,
2 — Phase $T-Al_9FeNi$,
3 — Phase $\pi-Al_8Mg_3FeSi_6$,
4 — Phase $\delta-Al_3CuNi$,
5 — Eutectic Al

2−4 intermetallic phases are observed at both solidification rates.

At the same time, it follows from Figs. 4 and 5 that the phases 4 and 5 appear only when scanning samples of alloys grown at a low velocity, 0.1 mm/s. At a speed of 0.8 mm/s, they don't have time to form. It should be noted that both phases contain Cu [15].

Figs. 4 and 5 show the latent heat of fusion (roughly proportional to volume) of all formations responsible for the appearance of the peaks. It can be seen that the melting enthalpy of the α Al + Si eutectic decreases with increasing silicon content in the alloy. When the silicon content increases by 5% in the alloy Al−15 wt.% Si−2 wt.% Cu, crystallized at a cooling rate of 0.1 mm/s, the enthalpy of melting of the eutectic decreases by 43% (Fig. 4, *a* and 5, *a*). In the case of the same alloy, but solidified at 0.8 mm/s, the enthalpy decrease with increasing silicon by 5% is 11% (Fig. 4, *b* and 5, *b*).

The decrease of αAl + Si eutectic content with increasing silicon content found here corresponds to the phase diagram in the area of hypereutectic silumin.

When the solidification rate of Al−15 wt.% Si−2 wt.% Cu increases from 0.1 to 0.8 mm/s (Fig. 4), the eutectic content of α Al + Si decreases slightly, by 3%. The total content of other hardening phases also decreases insignificantly, 4%.

When increasing the solidification rate of Al−20 wt.% Si−2 wt.% Cu from 0.1 to 0.8 mm/s (Fig. 5), the melting enthalpy of the αAl + Si eutectic increased

from 150 to 226 J/g and the total enthalpy of other observed hardening phases decreased from 427 to 342 J/g.

According to [9,17], the ultimate tensile strength of the Al−15 wt.% Si−2 wt.% Cu alloy studied here varies from 210 to 275 MPa depending on the solidification rate of 0.1 or 0.8 mm/s. At the same time, DSC shows a slight decrease in the volume of all observed hardening phases (Fig. 4). Based on this, it can be considered that the above increase in strength is determined by the decrease in the size of eutectic silicon during the transformation of the flake structure into a superfine nanofiber structure that is not optically resolvable (Fig. 1, *a, b*). This behavior has been extensively studied on binary silumins [7].

In the case of the alloy Al − 20 wt.% Si − 2 wt.% Cu, increasing the solidification rate from 0.1 to 0.8 mm/s causes the ultimate tensile strength to increase from 190 to 230 MPa (Fig. 6 in [9]). The total enthalpy of crystallization, proportional to the volume of all phases studied, falls by 2%. This means that the increase in strength is not determined by the volume of hardening phases, but by the change in structure. The change in the αAl + Si eutectic structure of the 20 wt.% Si alloy from rough, flaky to fine

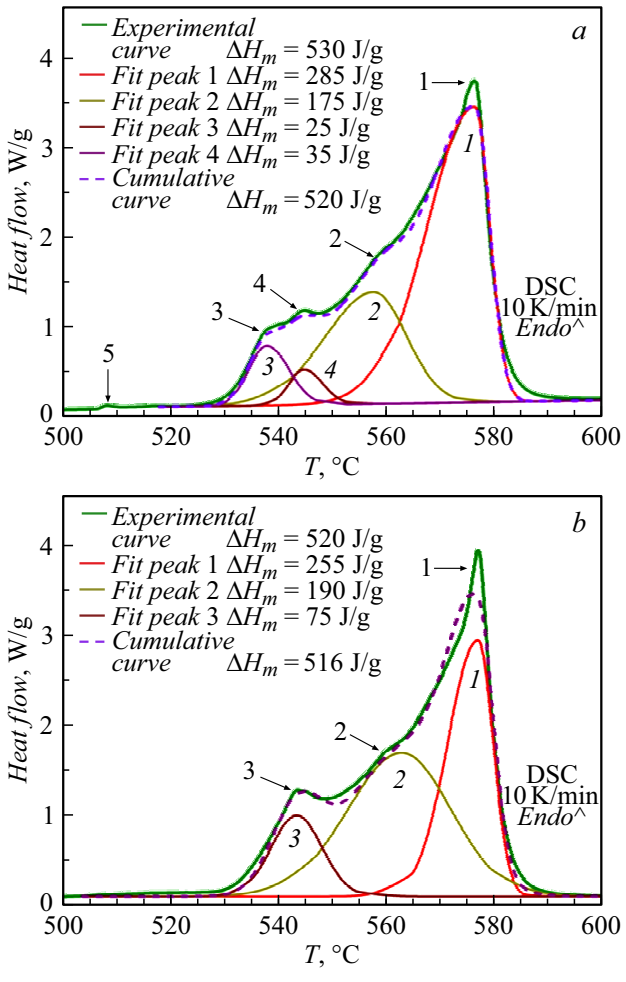

Figure 4. AlloyAl−15 wt.% Si−2 wt.% Cu: *a* — sample 1, $V = 0.1$ mm/s; *b* — sample 2, $V = 0.8$ mm/s (Table 2.).

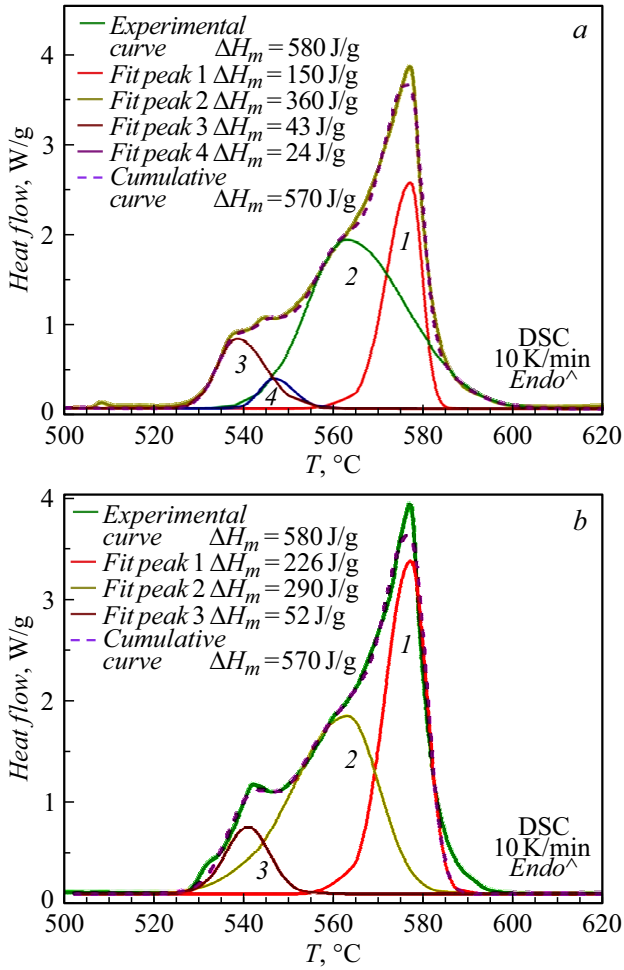

Figure 5. AlloyAl−20 wt.% Si−2 wt.% Cu: *a* — sample 5, $V = 0.1$ mm/s; *b* — sample 6, $V = 0.8$ mm/s (Table 2.).

nano-fibrous causes the observed change in ultimate tensile strength in the same way as in the 15 wt.% Si alloy.

It should be noted that the DSC of this work did not reveal melting of the αAl dendritic phase. (In work [4,15] the melting peak of aluminum was observed at 598 and 597−600°C.) The α Al-phase was not taken into account when estimating the strength change in terms of the volumes of the phases, which are roughly proportional to their enthalpies. According to [7] data, its strength, 110 MPa, is two and a half times lower than the strength of the eutectic α Al + Si, ∼ 250 MPa.

Conclusion

This paper analyzes the DSC curves of Al−xSi−2 wt.% Cu silumin alloys with 15, 17 and 20 wt.% silicon obtained by directional solidification at 0.1 and 0.8 mm/s. The role of both the eutectic volume and intermetallic compounds and the eutectic silicon microstructure in the variation of strength as a function of

solidification rate and silicon content in the Al − Si−Cu alloy is considered.

1. It is shown that the temperature of the maximum of DSC curves during melting and solidification of α-Al + Si eutectic alloy Al−xSi−2 Cu−1 Fe−1 Ni−0.7 Mg at x = 15, 17, 20 wt.% is 578 (melting) and 545°C (solidification) and is independent of the solidification rate of the alloy. The latent heat of fusion and crystallization of α-Al + Si eutectics in the area from 510 to 555°C and from 530 to 585°C increases with increasing silicon content.

2. The 5 peaks in the DSC curves during heating of alloys with 15 and 20 wt.% Si obtained at a solidification rate of 0.1 mm/s and 3 peaks at a rate of 0.8 mm/s were determined. It is shown that eutectic Al−Al_2Cu and phase δ-Al_3CuNi occurred only in alloys grown at low solidification rate 0.1 mm/s.

3. The melting enthalpy of the eutectics αAl + Si and Al−Al_2Cu and three intermetallic compounds was measured. Relative phase volumes roughly proportional to the enthalpy of fusion were used to approximate the ultimate tensile strength.

Conflict of interest

The authors declare that they have no conflict of interest.

References

[1] V.N. Osipov. ZhTF, **92** (9), 1365 (2022) (in Russian). DOI: 10.21883/JTF.2022.09.52928.42-22
[2] V. Vijiayan, N. Prabhu. C. Metall. Quarterly, **54** (1), 66 (2015). DOI: 10.1179/1879139514Y.0000000151
[3] C. Zhong-wei, Ma Cui-ying, C. Pey.Trans. Nonferrous Met. Soc. China, **22**, 42 (2012). DOI: 10.1016/S1003-6326(11)61137-0
[4] A. Luna, H. Mancha, M.J.C. Román, J.C.E. Bocardo, M.H. Trejo. Mater. Sci. Eng. A, **561**, 1 (2013). DOI: 10.1016/j.msea.2012.10.064
[5] M. Okayasu, S. Takeuchi, T. Ochi. Intern. J. Cast Metals Research, **30** (4), 217 (2017). DOI: 10.1080/13640461.2017.1286556
[6] G.K. Sigworth. Intern. J. Metalcasting, **2** (2), 19 (2008). DOI: 10.1007/BF03355425
[7] S.P. Nikanorov, L.I. Derkachenko, B.K. Kardashev, B.N. Korchunov, V.N. Osipov, V.V. Shpeizman. FTT, **55** (6), 1119 (2013). (in Russian).
[8] P.I. Antonov, L.M. Zatulovsky, A.S. Kostygov, D.I. Levinzon, S.P. Nikanorov, V.V. Peller, V.A. Tatarchenko, V.S. Yuferev. Preparation of profiled single crystals and products by the Stepanov method, ed. by V.R. Regel, S.P. Nikanorov (Nauka, L., 1981)
[9] S.P. Nikanorov, V.N. Osipov, R.B. Timashev, A.V. Chikiryaka. ZhTF **93**,(4), 554 (2023). DOI: 10.21883/JTF.2023.04.55044.202-22
[10] S. Pietrowsski. Mater. Design, **18** (4−6), 379 (1997). DOI: 10.1016/S0261-3069(97)00089-7
[11] Y. Sun, H. Cheng, N. Zhang, X.Tian. ISIJ Intern., **50** (12), 1875 (2010).
[12] J. Xu, S. Yu, E. Liu, H. Wang, S. Zhang. Mater. Sci. Forum, **787**, 6 (2014). DOI: 10.4028/www.scientific.net/MSF.787.6
[13] M.J. Starink. Intern. Mater. Rev., **49** (3−4), 192 (2004). DOI: 10.1179/095066004225010532
[14] G. Wang, X. Bian, W. Wang, J. Zhang. Mater. Lett., **57** (24−25), 4083 (2003). DOI: 10.1016/S0167-577X(03)00270-2
[15] M.H. Abdelaziz, E.M. Elgallad, H.V. Doty, S. Valtierra, F.H. Samuel. Philosophical Magazine, **99** (13), 1633 (2019). DOI: 10.1080/14786435.2019.1597993
[16] N.A. Belov, D.G. Eskin, N.N. Axentieva. Acta Mater., **53** (17), 4709 (2005). DOI: 10.1016/j.actamat.2005.07.003
[17] S.P. Nikanorov, V.N. Osipov, L.I. Regel. J. Mater. Eng. Perform., **28** (12), 7302 (2019). DOI: 10.1007/s11665-019-04414-3

Translated by Y.Deineka